A Novel Approach Using DFT to Explain the Selective Permeation of Small Gaseous Molecules through Y-Type Zeolite Membrane

Abhijit Chatterjee* and Takashi Iwasaki

Inorganic Materials Section, Tohoku National Industrial Research Institute, 4-2-1 Nigatake, Miyagino-ku, Sendai 983-8551, Japan

Received: May 4, 1999; In Final Form: August 5, 1999

The separation of individual component gases from a mixture of CO_2, N_2, CH_4, C_2H_6, and SF_6 along with the selective permeation of CO_2 from a mixture of CO_2/N_2 through Na-zeolite-Y membrane have been investigated using reactivity descriptors and interaction energy calculations by density functional theory (DFT). To locate the active site of zeolite-Y, three different cluster models are considered to propose the role of zeolite framework in the selectivity of gaseous molecular separation. All the interacting molecules were optimized with respect to the framework cluster to compare the stability of the adsorption complex. We have analyzed the effect of affinities of gas molecules for the membrane wall on the permeation to predict the optimal affinity strength, e.g., for higher selectivity of CO_2. We investigated the local softness of the interacting species with the zeolite framework cluster models. The order of activity as obtained from reactivity index values of individual molecules was compared with interaction energy calculations using DFT to validate the proposition. The result successfully predicts the experimental observation of selective permeation of gaseous molecules through Na-Y-zeolite pore in the order $C_2H_6 < CH_4 < SF_6 < CO_2 < N_2$ and also proposes the plausible mechanism of zeolite membrane functionality.

Introduction

With the advancement of technology environmental issues move from local level to global scale due to increasing industrial activities and production of new chemical materials. The problem which has generated the most attention is the global warming caused by the presence of gases such as carbon dioxide, methane, and chlorofluorocarbons in the environment. Among these gases, the presence of excess carbon dioxide in the atmosphere poses a serious threat to the global environment. Technologies are on the way to remove carbon dioxide from the atmosphere.[1,2] Direct separation processes are a convenient choice to remove carbon dioxide from the exhaust gases released from a particular stationary source, namely thermal power plants or fossil fuel combustion in large factories.[3] Materials of high thermal and chemical resistance are needed for such facilities, as the temperature of the exhaust gases is very high. Inorganic membranes, which contain subnanometer pores, are useful for the separation of gas mixtures under severe conditions where organic membranes are not functional.[4−6] Molecular sieving separation, which is performed by microporous materials like zeolite, is based on a much higher diffusion rate of the smallest molecule. Zeolites have been designed to separate hydrocarbon molecules.[7] MFI-type zeolite membrane formed on a ν-alumina-coated α-alumina porous tube, has been successfully used in the separation of *n*-octane, *i*-octane, and *n*-hexane[8]. To employ zeolite membranes in a practical manner, reproducibility in the membrane formation process is one of the most important factors. Funke et al.[9] reported that changes in membrane morphology occurred, for the same porous substrate, under different synthesis conditions. Kusakabe et al.[10] recently employed Y-type zeolite membrane and studied the permeances of single components and mixtures of CO_2 and N_2, as well as CH_4, C_2H_6, and SF_6. The separation of CO_2 is the most important industrial process in terms of its industrial application.

So far, there are many experimental and theoretical studies to monitor the interaction of gases with zeolite framework, but there is no effort so far to correlate the activity of the gas molecules in terms of interaction with zeolite framework. Now, the hard−soft acid−base (HSAB) principle classify the interaction between acids and bases in terms of global softness. Pearson proposed the global HSAB principle.[11] The global hardness was defined as the second derivative of energy with respect to the number of electrons at constant temperature and external potential, which includes the nuclear field. The global softness is the inverse of this. Pearson also suggested a principle of maximum hardness,[12] which states that, for a constant external potential, the system with the maximum global hardness is most stable. In recent days, DFT has gained widespread use in quantum chemistry. Some DFT-based local properties, e.g., Fukui functions and local softness,[13] have already been used for the reliable predictions in various types of electrophilic and nucleophilic reactions.[14−17] There are many recent studies which reveal that DFT-based reactivity descriptors can reproduce the experimentally observed protonation sites,[18] 1,3-dipolar cycloaddition,[19−21] reactivity of intermediates of the aromatic nucleophilic substitution,[22] and reactivity sequences of carbonyl compounds toward nucleophilic attack on them.[23] In our recent study,[24] we proposed a reactivity index scale for heteroatomic interaction with zeolite framework. Moreover, Gazquez and Mendez[25] proposed that when two molecules A and B of equal softness interact, thereby implicitly assuming one of the species as nucleophile and the other as an electrophile, then a novel bond would likely form between an atom A and an atom B whose Fukui function values are close to each other.

* Corresponding author. E-mail: chatt@tniri.go.jp. Phone: +81-22-237-5211. Fax: +81-22-236-6839.

10.1021/jp991453x CCC: $18.00
Published on Web 11/05/1999

The present study is in the area of zeolite membrane, which selectively separates gas molecules through permeation. We first use DFT-based local reactivity descriptors to correlate the activity of several gas molecules such as CO_2, N_2, CH_4, C_2H_6, and SF_6 with zeolite framework. Three different cluster models are considered to reproduce and compare the effect of environment on the activity of the active center present in zeolite framework. The reactivity indices of nucleophilic and electrophilic sites were compared. An activity order is proposed. The results were compared with the interaction energy calculations for each molecule with zeolite framework using DFT. The role of orientation of the molecule during permeation is also traced. A priori mechanism of the separation process through Y-type zeolite membrane was proposed.

Theory

Let us first recall the definition of various quantities employed. The Fukui function $f(r)$ is defined by[13]

$$f(r) = [\partial\mu/\partial v(r)]N = [\partial\rho(r)/\partial N]v \quad (1)$$

The function "f" is thus a local quantity, which has different values at different points in the species, and N is the total number of electrons. Since $\rho(r)$ as a function of N has slope discontinuities, eq 1 provides the following three reaction indices:[13]

$$f^-(r) = [\partial\rho(r)/\partial N]v \text{ (governing electrophilic attack)}$$

$$f^+(r) = [\partial\rho(r)/\partial N]v \text{ (governing nucleophilic attack)}$$

$$f^0(r) = 1/2[f^+(r) + f^-(r)] \text{ (for radial attack)}$$

In a finite difference approximation, the condensed Fukui function[26] of an atom, say x, in a molecule with N electrons are defined as

$$f_x^+ = [q_x(N+1) - q_x(N)] \text{ (for nucleophilic attack)}$$

$$f_x^- = [q_x(N) - q_x(N-1)] \text{ (for electrophilic attack)} \quad (2)$$

$$f_x^0 = [q_x(N+1) - q_x(N-1)]/2 \text{ (for radical attack)}$$

where q_x is the electronic population of atom x in a molecule. In density functional theory, hardness (η) is defined as[27]

$$\eta = 1/2(\partial^2 E/\partial N^2)v(r) = 1/2(\partial\mu/\partial N)\eta v$$

The global softness, S, is defined as the inverse of the global hardness, η.

$$S = 1/2\eta = (\partial N/\partial\mu)v$$

The local softness $s(r)$ can be defined as

$$S(r) = (\partial\rho(r)/\partial\mu)v \quad (3)$$

Equation 3 can also be written as

$$S(r) = [\partial\rho(r)/\partial N]v[\partial N/\partial\mu]v = f(r)S \quad (4)$$

Thus, local softness contains the same information as the Fukui function $f(r)$ plus additional information about the total molecular softness, which is related to the global reactivity with respect to a reaction partner, as stated in HSAB principle. Using the finite difference approximation, S can be approximated as

$$S = 1/(\mathrm{IE} - \mathrm{EA}) \quad (5)$$

where IE and EA are the first ionization energy and electron affinity of the molecule, respectively. Atomic softness values can easily be calculated by using eq 4, namely,

$$s_x^+ = [q_x(N+1) - q_x(N)]S$$

$$s_x^- = [q_x(N) - q_x(N-1)]S \quad (6)$$

$$s_x^0 = S[q_x(N+1) - q_x(N-1)]/2$$

Computational Methodology and Model

In the present study, all calculations have been carried out with DFT[28] using DMOL code of MSI Inc. BLYP[29,30] exchange correlation functional and DNP basis set[31] was used throughout the calculation. BLYP has already shown its credibility for explaining weak hydrogen bond type interactions in comparison to MP2 level calculations.[32,33] It is also useful in describing the interaction of heteroatomic molecules with zeolite framework cluster.[24] Basis set superposition error (BSSE) was also calculated for the current basis set in nonlocal density approximation (NLDA) using Boys−Bernardi method.[34] Geometries of all the interacting gaseous molecules CO_2, N_2, CH_4, C_2H_6, and SF_6 along with the zeolite framework cluster models representing the three different gateways of Y-type zeolite were fully optimized for calculating the reactivity index. The theory of reactivity index calculations is mentioned elsewhere in detail.[24] Single-point calculations of the cation and anion of each molecule at the optimized geometry of the neutral molecule were also carried out to evaluate Fukui functions and global and local softness. The condensed Fukui function and atomic softness were evaluated using eqs 2 and 6, respectively. The gross atomic charges were evaluated by using the technique of electrostaic potential (ESP) driven charges. It is well-known that Mulliken charges are highly basis set dependent, whereas ESP driven charges show less basis set dependence[35,36,24] and are better descriptors of the molecular electronic density distribution. Calculations have been performed on three different clusters with formula (a) $NaSiAlO_7H_6$, (b) $NaSi_2Al_2O_{13}H_{11}$, and (c) $NaSi_5AlO_{18}H_{12}$. The adjacent silicon and aluminum atoms occurring in the zeolite lattice are replaced by hydrogens to preserve the electroneutrality of the model as shown in Figure 1a−c. The terminal hydrogens are kept at a distance of 1.66 Å. The aim of the present communication is to use DFT-based reactivity descriptors to compare the local softness values of the atoms of the interacting molecules along with the zeolite framework cluster. The atoms for which those values will be closer will be considered as the most probable sites of interaction. Then the proposition will be justified and the mechanism from interaction energy calculations will be proposed.

Results and Discussion

The global softness values of the zeolite cluster models as well as the interacting molecules calculated using DFT are presented in Table 1. The global hardness values of the clusters are mentioned at the bottom of the table for comparison. The values of nucleophilic condensed local softness (s_x^+) and condensed Fukui function (f_x^+) of the individual atoms of the cluster models obtained through the ESP technique at the DFT level are shown in Table 2. The electrophilic condensed local softness (s_x^-) and condensed Fukui function (f_x^-) have been calculated for all the interacting molecules using ESP method and presented in Table 3. It is observed from Table 1, that those global softness values for the zeolite cluster models are higher than that of the interacting molecular species. So to test the

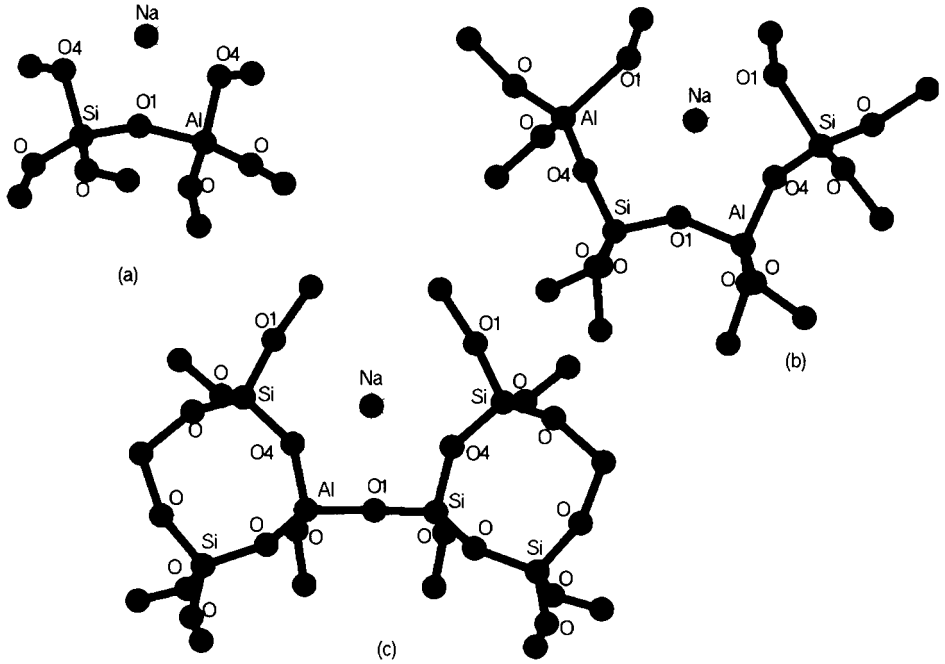

Figure 1. Sketch of framework cluster models with formula (a) $NaSiAlO_7H_6$, (b) $NaSi_2Al_2O_{13}H_{11}$, and (c) $NaSi_5AlO_{18}H_{12}$. All the atoms are labeled except the hydrogens for visual clarity. Only the oxygens directly interacting with the molecule are labeled according to their type (O1/O4).

TABLE 1: Global Softness Values (in au) for Zeolite Cluster along with Different Gaseous Interacting Molecules[a]

molecule	global softness (au)
framework cluster a	2.9188
framework cluster b	7.0472
framework cluster c	8.5616
carbon dioxide	1.7663
nitrogen	1.4920
methane	1.5909
ethane	1.9306
hexafluoro sulfur	1.2706

[a] Global hardness (in au) for the zeolite clusters is (a) 0.1713, (b) 0.0709, and (c) 0.0584.

HSAB principle, it seems to be important to analyze whether the local softness values, Fukui functions, or reactive indices for the constituent atoms of the cluster models and interacting molecular species will be more reliable parameters. First, the interaction of the zeolite cluster models with each of the five probe molecules is calculated using local softness values and an activity order is proposed. This is compared with existing experimental permittivity order. Then, the effect of cluster size in explaining the activity order is compared and finally the interaction energy of the individual molecule with the best zeolite framework cluster model was carried out to justify the proposed order.

The result has always been monitored in terms of the experimental permeation results to validate the experimental selectivity. Finally, from all the results a plausible mechanism of the permeation of gases through zeolite membrane is proposed.

a. Effect of Cluster Size on Reactivity Descriptors. Zeolites are crystalline aluminosilicates consisting of SiO_4 and AlO_4^- tetrahedra, linked in such a way as to form cages and channels of molecular dimensions. The structure of zeolite Na−Y, determined from neutron diffraction data, was recently reported by Fitch et al.[37] The space group is *fd*3*m* with a lattice parameter $a = 24.85$ Å. The framework is composed of cubooctahedral sodalite cages linked together in a tetrahedral arrangement by six-membered rings of O1 atoms to form large cavities, called supercages. The supercages are interconnected by windows that are formed by rings consisting of 12 Si/Al and 12 O atoms (Figure 2). The probable locations of extraframework cations

TABLE 2: Condensed Fukui Function and Local Softness Values for Zeolite Cluster Models (Only the Oxygens of the Cluster Interacting with Molecules are Labeled)

atoms of (a)	ESP technique f_x^+	ESP technique s_x^+	atoms of (b)	ESP technique f_x^+	ESP technique s_x^+	atoms of (c)	ESP technique f_x^+	ESP technique s_x^+
O1	0.10	0.291	O1	0.02	0.141	O1	0.02	0.171
O4	0.06	0.175	O	0.04	0.282	O4	0.01	0.085
O	0.03	0.087	O	0.02	0.141	O	0.03	0.257
O4	0.05	0.145	O4	0.01	0.070	O	0.01	0.085
O	0.04	0.116	O1	0.02	0.141	O1	0.02	0.171
O1	0.08	0.233	O	0.02	0.141	O4	0.01	0.085
O	0.03	0.087	O	0.02	0.141	O	0.02	0.171
H	0.06	0.175	O4	0.01	0.070	O	0.01	0.085
H	0.05	0.145	O1	0.01	0.070	O1	0.02	0.171
H	0.08	0.233	O	0.01	0.070	O	0.02	0.171
H	0.05	0.145	O	0.02	0.141	O	0.03	0.257
H	0.07	0.204	O	0.02	0.141	O	0.02	0.171
H	0.11	0.321	O	0.02	0.141	O	0.02	0.171
Si	0.07	0.204	H	0.05	0.352	O	0.02	0.171
Al	0.07	0.204	H	0.07	0.493	O	0.01	0.085
Na	0.12	0.350	H	0.07	0.493	O	0.01	0.085
			H	0.06	0.423	O	0.01	0.085
			H	0.06	0.423	O	0.02	0.171
			H	0.08	0.563	O	0.03	0.257
			H	0.06	0.423	H	0.03	0.257
			H	0.07	0.493	H	0.04	0.342
			H	0.05	0.352	H	0.04	0.342
			H	0.07	0.493	H	0.03	0.257
			H	0.05	0.352	H	0.06	0.514
			Si	0.07	0.493	H	0.05	0.428
			Si	0.07	0.493	H	0.06	0.514
			Al	0.06	0.423	H	0.05	0.428
			Al	0.07	0.493	H	0.06	0.514
			Na	0.09	0.634	H	0.06	0.514
						H	0.05	0.428
						H	0.04	0.342
						Si	0.03	0.257
						Si	0.01	0.085
						Si	0.02	0.171
						Si	0.02	0.171
						Si	0.03	0.257
						Al	0.02	0.171
						Na	0.08	0.684

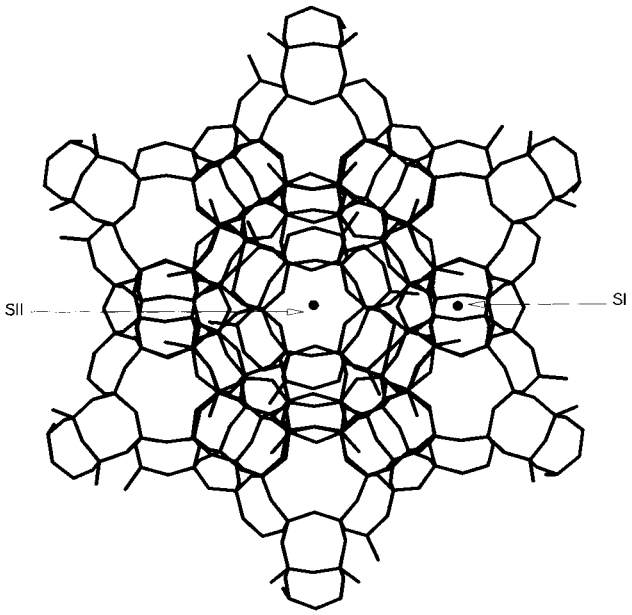

Figure 2. Sketch of supercage of zeolite Na−Y with the cation positions. The SI site is located at the centers of the hexagonal prism; the positions of SII sites are in the supercages. The T atoms are located at the vertices.

TABLE 3: Condensed Local Softness and Fukui Functions for All the Interacting Gaseous Molecules

atoms of interacting molecules	ESP technique	
	f_x^-	s_x^-
C in CO_2	0.2809	0.4961
O in CO_2	0.3547	0.6265
N in N_2	0.0512	0.7460
C in CH_4	0.1612	0.2564
H in CH_4	0.2043	0.3250
C in C_2H_6	0.0275	0.0532
H in C_2H_6	0.1575	0.3049
S in SF_6	0.2873	0.3650
F in SF_6	0.2146	0.2726

are SI and SII as shown in Figure 2. To model the typical architecture we considered three different clusters as shown in Figure 1 and described in earlier section. As we have observed earlier,[38] there are two different oxygens present in zeolite-Y, so based on that we also justified the location of sodium on the cluster. This is also supported by the crystallographic structure results by Bergerhoff et al.[39] who have shown for the first time the presence of four different crystallographic oxygens present in Y-type zeolite. Here, in our models the oxygens directly interacting with the framework were labeled as O1/O4 as the case may be. The model structure has been used for a more realistic picture for Y-type zeolite crystals (though it is limited by the fact that the model is an approximation of the actual crystal). In several other theoretical studies,[40,41] the structure of the cluster model is generated by geometry optimization at some level of sophistication. All the structures were fully optimized for calculating the reactivity parameters, so they neither depict a particular site of the zeolite framework nor reflect the actual experimental situation (environment) but could mimic the system in the best possible way. In the optimized clusters the Na−O distance is ∼2.38 Å. The effect of cluster size was monitored. The global softness values for the zeolite clusters show an increase with the size of the cluster, as shown in Table 1. The value of global hardness shown in the bottom of the table shows a reverse trend; that is, with increase in the size of cluster the global hardness decreases. The effect of Si/Al ratio and other parameters has not been monitored here. Now, in all these clusters, Na is occupying either the SI or SII site as shown in Figure 2, as it happens to be in the structure. The local parameters, Fukui function, and atomic softness values show a reverse order, as anticipated from chemical intuition. The charge on sodium is dissipated to its surroundings with increase in the cluster size. The charge delocalization is observed from the reactivity descriptors values as obtained from ESP charges generated from DFT. With the increase in cluster size the environment is also changing which results in different charge delocalization as observed from the values of the reactivity descriptors as they are generated from the net charges calculated by ESP methodology. It is also observed that the active site of the zeolite cluster is the sodium, which may be termed as extraframework cation. In all the clusters we assumed only one sodium per framework cluster. The first two clusters (a and b) are demonstrating the small pore entry region, i.e., SII site, while the third cluster (c) depicts the entry point along with it surroundings as present inside the supercage i.e., site SI as shown in Figure 2. The results show that c will be the best choice for further calculation as it is the best cluster model to reproduce the environment of the active center.

b. Interaction of Zeolite Cluster with CO_2/N_2. This is to correlate the activity of the atoms of gas molecules with that of active cation center of zeolite. The global softness values in Table 1 show that the global softness of CO_2 is much higher than that of N_2, where as the Fukui function (f_x^-) and atomic softness (S_x^-) of the constituent atoms show that nitrogen is more active in comparison to that of carbon and oxygen. In other words, nitrogen is more nucleophilic than carbon and oxygen of carbon dioxide. It is observed for the smaller cluster (a), the most nucleophilic atom for CO_2 is carbon with respect to most nucleophilic atom of the zeolite cluster Na atom. Which is different from that for clusters (b) and (c), now our observation is that this behavior is dependent on the cluster size or in another way on the environment of the active site, which is not truly mimicked in cluster (a) but is realistic in clusters (b) and (c). In carbon dioxide, oxygen is more nucleophilic than carbon. The most nucleophilic atom will be attracted by the most electophilic moiety of zeolite cluster, which is in all the three cases the extraframework cation sodium as observed from the f_x^+ and s_x^+ values presented in Table 2. Experimentally, it is observed that during permeation carbon dioxide has a better permeance in comparison to that of nitrogen. The stronger nitrogen adsorption in zeolite matrices is also been observed by Papai et al.[42] The interaction of smaller molecules with a positive point charge has demonstrated that a classical description involving electrostatic and induction energies, which depend respectively on their quadruple moment and dipole polarizability, is adequate to explain the basic reason for a stronger nitrogen adsorption. This observation so far can be validated by HSAB principle. We will further justify the permeation selectivity by interaction energy calculations and will propose the plausible mechanism.

c. Interaction of the Zeolite Cluster Model with CH_4, C_2H_6, and SF_6. The interaction of these gaseous molecules with zeolite framework has been tested to validate the model. In real experiment, these gases are used in the feed in a process of separation as mentioned in the experimental results of Kusakabe et al.[10] The global softness values present in Table 1 show that the activity order is $C_2H_6 > CH_4 > SF_6$. Now we compare the f_x^- and s_x^- values for the constituent atoms of all three molecules; the results are presented in Table 3. The results show that in methane the most nucleophilic atom is hydrogen, that means hydrogen of methane will approach the most electrophilic site of zeolite, i.e., sodium. In the case of ethane the scenario is

TABLE 4: Comparison of Condensed Local Softness and Fukui Functions of the Most Nucleophilic Atom of the Interacting Gaseous Molecules

atom of interacting gaseous molecules	f_x^-	s_x^-
O in CO_2	0.3547	0.6265
N in N_2	0.4988	0.6337
H in CH_4	0.2043	0.3250
H in C_2H_6	0.1575	0.3049
S in SF_6	0.2873	0.3650

the same. Hydrogen having the higher value of f_x^- and s_x^- will approach the sodium of zeolite cluster, which has highest f_x^+ and s_x^+ values. The situation is totally different in the case of hexafluoro sulfur. The Fukui function and local softness values show that S in SF_6 is more nucleophilic than the F present. So in this case, hexafluoro sulfur will act as the nucleophilic active site while interacting with the electrophilic center of zeolite, i.e., sodium. The possibility of electrophilic attack on SF_6 has been confirmed by its reaction with certain Lewis acids.[43] The orientation of the optimized SF_6 molecule over the zeolite cluster is discussed in the following section. Now as SF_6 is octahedral while interacting with the framework cluster it undergoes some distortion to allow the pseudobond formation between its nucleophilic center and the electrophilic center of the zeolite in the domain of HSAB principle.

d. Reactivity Index Scale. One of the aims of the current study is to rationalize an understanding of the permeation of gaseous molecules through zeolite pores. As the rate of permeation is dependent on the rate of interaction or in another way how strongly the molecule interacts with the zeolite framework, that will determine which molecule will pass more easily through the zeolite membrane. This permeation is dependent on pore architecture as well as on the interaction of molecules with the zeolite framework. Now to explore this we first tried to find an order of activity of the gaseous molecules in terms of reactivity index. It is observed from Table 1 that the zeolite framework has a higher value for global softness in comparison to interacting molecules. The order of global softness for the interacting molecules in comparison to framework cluster is $SF_6 < N_2 < CH_4 < C_2H_6 < CO_2$. Now, we present the results of condensed softness and Fukui functions of the most nucleophilic atom of the interacting molecules from the ESP technique at the DFT level in Table 4. The results show that in terms of Fukui functions and condensed local softness the interacting molecules can be arranged in the order $C_2H_6 < CH_4 < SF_6 < CO_2 < N_2$. Now, here we observed from the results shown in Table 4, that individual f_x^- and s_x^- values for the constituent atoms of interacting molecules are widely different, which clearly shows that only one atom of the interacting molecule is active in comparison to the other. In our earlier publication,[24] we have shown that in a situation like this the reactivity order will act as a scale, which can be validated by interaction energy calculations. Thus, there will be unisite interaction, i.e., the most nucleophilic site of the molecule interacts with the most electrophilic site of the zeolite framework cluster. Now to verify this order we need to perform interaction energy calculation using DFT.

e. Interaction Energy Calculation. The interaction energy calculation was performed using DFT with the BLYP functional. The validity of the current methodology in predicting the interaction energy is tested with a small model calculation with H_2O-H_2O and H_2O-HF systems. The results were compared with existing results obtained from MP2 level calculations.[33,44] The results are tabulated in Table 5. It shows that our current methodology can reproduce the binding energy of the smaller

TABLE 5: BLYP and MP2 Binding Energy Results for H_2O-H_2O and H_2O-HF Using a Similar Basis Set [6-31++G(d,p) for MP2; DNP for BLYP[a]

	MP2		BLYP	
system	BE (kcal/mol)	BE (BSSE) (kcal/mol)	BE (kcal/mol)	BSSE (kcal/mol)
H_2O-H_2O[b]	−5.24	−4.47	−5.01	−4.54
H_2O-HF[c]	−10.15	−8.13	−9.98	−8.76

[a] BE = binding energy; BE (BSSE) = BSSE corrected binding energy. [b] Results in ref 33. [c] Results in ref 44.

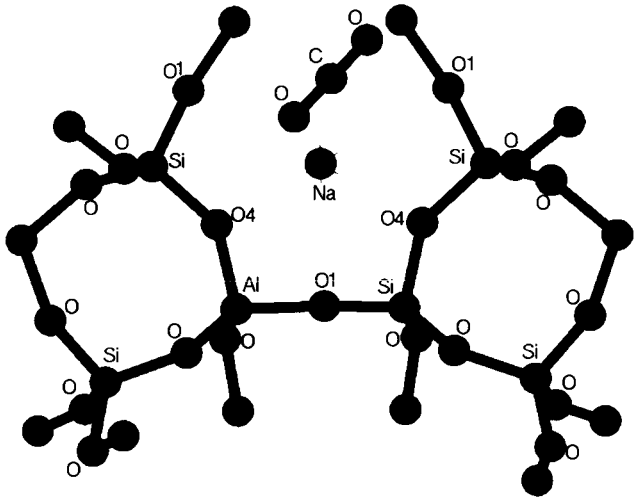

Figure 3. Optimized structure of carbon dioxide molecule during interaction with zeolite framework cluster model (c).

models with an error of ±0.01 kcal/mol. Now, for the interaction energy calculation, the framework cluster "c" was chosen, as it considers the environment of sodium most realistically. The framework cluster was kept fixed and the interacting molecules were fully optimized. For each case, the most nucleophilic atom (as observed from the reactivity index values) of the interacting molecules was placed at a distance of 2 Å from the active sodium of the zeolite framework. Since a linear Na^+-molecule geometry is the most favorable in the gaseous state,[42] the incoming molecules were approached to site II (SII) cations along the pseudo-C_3 axis of the six-membered ring, yielding the optimum distances to Na^+; the interatomic bond lengths of interacting molecules kept fixed at their equilibrium values optimized for isolated Na^+-N_2 (1.095 Å). The orientation of the incoming molecules has thus been adjusted, minimizing the van der Waals repulsion with the neighboring atoms.[45] The optimized configurations of carbon dioxide, nitrogen, and SF_6 with respect to the framework cluster "c" are shown in Figures 3, 4, and 5, respectively. The results of the total energy of the framework cluster and the individual interacting molecules along with the adsorption complex and interaction energy (BSSE corrected) are shown in Table 6. Now, as we mentioned earlier, in all the cases the orientation of the interacting molecules with the framework shows that parallel to the framework is the most stable configuration with a tilt toward the sodium cation. We varied the starting configurations, starting from perfectly parallel to perpendicular, and optimized for each case. The global minima for each molecule with respect to the framework are tabulated. The interaction energy values fall in the range 2.23−9.65 kcal/mol. We will not emphasize the numerical values; rather we will explore the trend. The interaction energy values show the order as $C_2H_6 < CH_4 < SF_6 < CO_2 < N_2$. This trend matches perfectly with the order proposed by the reactivity index in the earlier section. This validates our earlier proposition that,

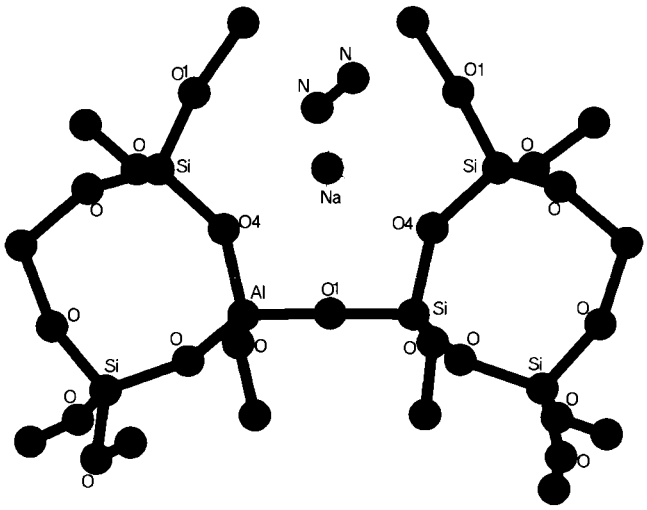

Figure 4. Optimized structure of nitrogen molecule during interaction with zeolite framework cluster model (c).

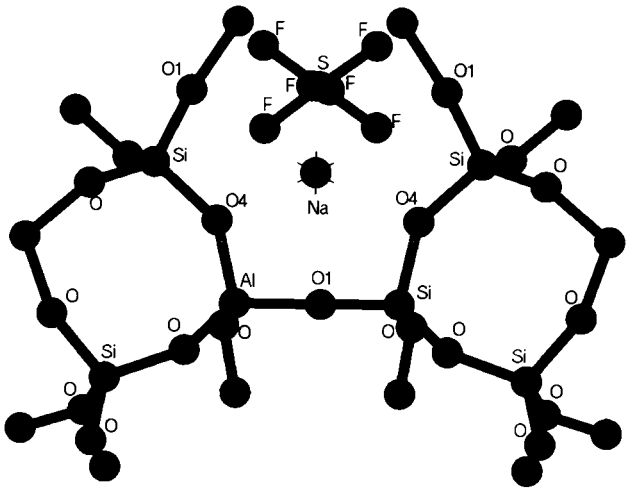

Figure 5. Optimized structure of hexafluoro sulfur molecule during interaction with zeolite framework cluster model (c).

TABLE 6: Total Energy of the Framework and Interacting Gaseous Molecules along with Interaction Energy for Each of the Individual Interacting Molecules with Zeolite Framework at Their Optimized Configuration

molecule and cluster	total energy (au)	interaction energy (kcal/mol) BSSE corrected
nitrogen	−108.679	
carbon dioxide	−187.263	
hexafluoro sulfur	−997.408	
methane	−40.490	
ethane	−79.783	
framework cluster c	−3271.361	
FW + nitrogen	−3380.055	−9.65
FW + carbon dioxide	−3458.635	−7.13
FW + hexafluoro sulfur	−4268.777	−5.32
FW + methane	−3311.857	−3.98
FW + ethane	−3351.147	−2.23

for unisite interaction, the reactivity index scale is the best predictor for the interaction of molecules. So from the DFT-based local parameter descriptor, one can conclusively locate the active site in the interacting molecular species, and by comparing with the parametric value for zeolites one can choose the best plausible candidate for a particular type of reaction.

f. Mechanism of Permeation. The most challenging part for the experimentalist is the separation of carbon dioxide and nitrogen from the mixture. According to the experimental observation, the permeance mechanism is not well understood. They predicted that the permeation mechanism of the Y-type membrane is different from the macroporous membrane. The free aperture of the main channels in Y-type zeolite is 7.4 Å and is much larger than the diameters of all the interacting molecules including carbon dioxide and nitrogen. If the concentrations of CO_2 and N_2 in the micropores of the Y-type zeolite membrane are equal to those in the outside gas phase, these molecules permeate through the membrane at a low CO_2/N_2 selectivity. However, this is not the case. The results obtained from interaction energy calculations shows that nitrogen forms the strongest adsorption complex in comparison to other gaseous molecules, so the nitrogen gets stabilized inside the pore and the carbon dioxide permittivity increases. Now, the permeation takes place through the smaller six-member pore opening which gradually gets saturated with the increase in the concentration of the gas mixture. This problem is solved with the increase of temperature. It is observed experimentally[10] that the permeance of SF_6 was higher than that of CH_4 and N_2, so our calculation mimicked the situation with nice accuracy. The experimental observation of the fact that nitrogen permeation occurs through a nonadsorptive translation−collision mechanism goes against the proposition of these results. Nonadsorptivity does not occur in the case of nitrogen as observed in the results. Actually, when the rate of permeance gets slower by the accumulation of carbon dioxide, then it is misleading with reagard to the adsorptivity. We validate our proposition with the reactivity parameter as well as the interaction energy results.

Conclusion

This is the first study to rationalize the understanding between selective permeation of gaseous molecules through zeolite membrane in terms of reactivity index and is validated by interaction energy calculations using DFT. Though this is not a quantitative study, we claim that the findings which are qualitative in terms of their numerical output are a novel approach in solving the permeation process of a smaller molecule through zeolite membrane. The novelty lies in the simplicity of the approach, which is so far the only plausible way to explain the mechanism of the permeation process. The results validate our earlier[24] proposition that for molecules with one active site, i.e., nucleophilic site can preferentially interact with most electrophilic site of the interacting material (e.g., zeolite), the reactivity descriptors can conclusively predict the selectivity of the interacting molecules with respect to a particular interacting matrix. Experimentally, the selectivity of carbon dioxide over nitrogen is clearly understood. The current results also propose the mechanism of the permeation, which logically defers from the experimental prediction of nonadsorptivity of nitrogen. The results show that nitrogen forms the strongest adsorption complex, which further helps in the migration of other gases through zeolite pores. Zeolite clusters are rationally modeled to consider the environment of the active cation, which realistically considers the experimental situation. The optimistic result paves a novel way of explaining reactive centers in a particular reaction, which can eliminate tedious experimentation.

References and Notes

(1) Suda, T.; Fujii, M.; Yoshida, K.; Iijima, M.; Seto, T.; Mitsuoka, S. *Energy Convers. Manage.* **1992**, *33*, 317.

(2) Niswander, R. H.; Edwards, D. J.; DuPart, M. S.; Tse, J. P. *Sep. Sci. Technol.* **1993**, *28*, 565.

(3) Cogbill, M. J.; Marsh, G. P. *Energy Convers. Manage.* **1992**, *22*, 487.

(4) Gavalas, G. R.; Megiris, C. E.; Nam, S. W. *Chem. Eng. Sci.* **1989**, *44*, 1829.
(5) Yan, S.; Maeda, H.; Kusakabe, K.; Morooka, S.; Akiyama, Y. *Ind. Eng. Chem. Res.* **1994**, *33*, 2096.
(6) Morooka, S.; Yan, S.; Kusakabe, K.; Akiyama, Y. *J. Membr. Sci.* **1995**, *101*, 89.
(7) van Bekkum, H.; Geus, E. R.; Kouwenhoven, H. W. In *Advanced Zeolite Science and Applications*; Jansen, J. C., Stocker, M., Karge, H. G., Weitkemp, J., Eds.; Elsevier: Amsterdam, The Netherlands, 1994; pp 509−542.
(8) Yan, Y.; Tsapatsis, M.; Gavalas, G. R.; Davis, M. E. *J. Chem. Soc., Chem. Commun.* **1995**, 227.
(9) Funke, H. H.: Kovalchick, M. G.; Falconer, J. L.; Noble, R. D. *Ind. Eng. Chem. Res.* **1996**, *35*, 1575.
(10) Kusakabe, K.; Kuroda, T.; Murata, A.; Morooka, S. *Ind. Eng. Chem. Res.* **1997**, *36*, 649.
(11) Pearson, R. G. *J. Am. Chem. Soc.* **1983**, *105*, 7512.
(12) Pearson, R. G. *J. Chem. Educ.* **1987**, *64*, 561.
(13) Parr, R. G.; Yang, W. *J. Am. Chem. Soc.* **1984**, *106*, 4049.
(14) Langenaeker, W.; Demel, K.; Geerlings, P. *J. Mol. Struct. (THEOCHEM)* **1992**, *259*, 317.
(15) Langenaeker, W.; Proft, F. De.; Geerlings, P. *J. Phys. Chem.* **1995**, *99*, 6624.
(16) Langenaeker, W.; Proft, F. De.; Geerlings, P. *J. Phys. Chem. A* **1998**, *102*, 5944.
(17) Chandra, A. K.; Geerlings, P.; Nguyen, M. T. *J. Org. Chem.* **1997**, *62*, 6417.
(18) Roy, R. K.; Proft, F. De.; Geerlings, P. *J. Phys. Chem. A* **1998**, *102*, 7035.
(19) Chandra, A. K.; Nguyen, M. T. *J. Comput. Chem.* **1998**, *19*, 195.
(20) Mendez, F.; Tamariz, J.; Geerlings, P. *J. Phys. Chem. A* **1998**, *102*, 6292.
(21) Chandra, A. K.; Nguyen, M. T. *J. Phys. Chem. A* **1998**, *102*, 6181.
(22) Langenaekar, W.; Proft, F. D.; Geerlings, P. *J. Phys. Chem. A* **1998**, *102*, 5944.
(23) Roy, R. K.; Krishnamurthy, S.; Geerlings, P.; Pal, S. *J. Phys. Chem. A* **1998**, *102*, 3746.
(24) Chatterjee, A.; Iwasaki, T.; Ebina, T. *J. Phys. Chem. A* **1999**, *103*, 2489.
(25) Gazquez, J. L.; Mendez, F. *J. Phys. Chem.* **1994**, *98*, 4591.
(26) Yang, W.; Mortier, M. J. *J. Am. Chem. Soc.* **1986**, *108*, 5708.
(27) Pearson, R. G.; Parr, R. G. *J. Am. Chem. Soc.* **1983**, *105*, 7512.
(28) Kohn, W.; Sham. L. J. *Phys. Rev. A* **1965**, *140*, 1133.
(29) Becke, A. *J. Chem. Phys.* **1988**, *88*, 2547.
(30) Lee, C.; Yang, W.; Parr, R. G. *Phys. Rev. B* **1988**, *37*, 786.
(31) Bock, C. W.; Trachtman, M. *J. Phys. Chem.* **1994**, *98*, 95.
(32) (a) Sim, F.; St-Amant, A.; Papai, I.; Salahub, D. R. *J. Am. Chem. Soc.* **1992**, *114*, 4391. (b) Kim, K.; Jordan, K. D. *J. Phys. Chem.* **1994**, *98*, 10089.
(33) Chandra, A. K.; Nguyen, M. T. *Chem. Phys.* **1998**, *232*, 299.
(34) Boys, S. F.; Bernardi, F. *Mol. Phys.* **1970**, *19*, 553.
(35) Proft, F. D.; Martin, J. M. L.; Geerlings, P. *Chem. Phys. Lett.* **1996**, *250*, 393.
(36) Geerlings, P.; Proft, F. D.; Martin, J. M. L. In *Recent Developments in Density Functional Theory; Theoretical and Computational Chemistry 5*; Seminario, S., Ed.; Elsevier: Amsterdam, 1996; pp 773−780.
(37) Fitch, A. N.; Jobic, H.; Renouprez, A. *J. Phys. Chem.* **1986**, *90*, 1311.
(38) Chatterjee, A.; Iwasaki, T.; Ebina, T.; Tsuruya, H.; Kanougi, T.; Oumi, Y.; Kubo, M.; Miyamoto, A. *Appl. Surf. Sci.* **1998**, *130−132*, 555.
(39) Bergerhoff, G.; Baur, W. H.; Nowacki, W.; Jahrab, N. *Neues Jahrab. Mineral.* **1958**, *9*, 193.
(40) van Santen, R. A.; Kramer, G. J. *Chem. Rev.* **1995**, *95*, 637.
(41) Sauer, J. *Chem. Rev.* **1989**, *89*, 199.
(42) Papai, I.; Goursot, A.; Fajula, F.; Plee, D.; Weber, J. *J. Phys. Chem.* **1995**, *99*, 12925.
(43) Cotton, F. A.; Wilkinson, G. *Advanced Inorganic Chemistry*, 5th ed.; John Wiley & Sons: New York, 1988; pp 510−511.
(44) Novoa, J. J.; Planas, M.; Rovira, M. C. *Chem. Phys. Lett.* **1996**, *251*, 33.
(45) Goursot, A.; Vasilyev, V.; Arbuznikov, A. *J. Phys. Chem. B* **1997**, *101*, 6420.